Available online at www.sciencedirect.com
SCIENCE DIRECT
Journal of Power Sources 147 (2005) 184–195
JOURNAL OF POWER SOURCES
www.elsevier.com/locate/jpowsour

Water and thermal management for Ballard PEM fuel cell stack

Xiaochen Yu, Biao Zhou *, Andrzej Sobiesiak

Department of Mechanical, Automotive and Materials Engineering, University of Windsor, Windsor, Ont., Canada N9B 3P4

Received 31 December 2004; accepted 27 January 2005
Available online 8 March 2005

Abstract

A water and thermal management model for a Ballard PEM fuel cell stack was developed to investigate its performance. A general calculation methodology was developed to implement this model. Knowing a set of gas feeding conditions (i.e., pressure, temperature, flow rate) and stack physical conditions (i.e., channel geometry, heat transfer coefficients, operating current), the model could provide information regarding the reaction products (i.e., water and heat), stack power, stack temperature, and system efficiency, thereby assisting the designer in achieving the best thermal and water management. Furthermore, if the stack undergoes a perturbation, such as the initial start-up, quick change in current, or a shutdown, the model could predict the dynamic information regarding stack temperature, cell voltage, and power as a function of time.

Keywords: Two-phase model; Fuel cell; Relative humidity; Exit temperature; Steady model; Transient model

1. Introduction

A proton exchange membrane (PEM) fuel cell is an electrochemical device where the energy of a chemical reaction is converted directly into electricity, by combining hydrogen fuel with oxygen from air [1]. Water and heat are the only by-products if hydrogen is used as the fuel source for PEM fuel cell. Most of the current research and development efforts focus on PEM fuel cells due to their capability of higher power density and faster start-up than other fuel cells [2–6]. Usually PEM fuel cells could be operated at a temperature lower than 100 °C, thus faster start-up and immediate response to changes in the demand for power could be realized.

Water and thermal management has become one of the key technical challenges that must be resolved in order for the PEM fuel cell technology to be feasible for transportation applications [7,8], although, over the last decade, significant progress has been made in the field of PEM fuel cell stack development [9–11]. Proper water and thermal management is essential for optimizing the performance of a fuel cell stack.

In automotive applications, there are many different road conditions involved and therefore the knowledge on the PEM fuel cell stack in terms of steady and transient behavior (e.g., acceleration, deceleration) becomes very important. In an automotive fuel cell stack, water and thermal management on this steady and transient behavior is associated with many parameters that affect the design and performance of PEM fuel cell. In order to understand the relative importance of the parameters and their interaction, an investigation on these parameters is required [12]. Mathematical modeling, a convenient and powerful technique, is therefore well suited for this task. The numerical modeling could be employed to significantly reduce the time and cost associated with the PEM fuel cell stack development.

To date, most of the work done in terms of PEM fuel cell modeling has focused on the electrochemical and diffusion processes of individual fuel cell (also called unit cell). Some noteworthy early examples include Dunbar and Gaggioli [13], Springer et al. [14], Verbrugge and Hill [15], Bernardi and Verbrugge [16,17], Fuller and Newman [18], Nguyen and White [19] and Kim et al. [20]. University of Victoria and University of Waterloo [21–25] have been conducting the fuel cell modeling for many years and have made very impressive progress on the unit cell modeling.

* Corresponding author. Tel.: +1 519 253 3000x2630; fax: +1 519 973 7007.
E-mail address: bzhou@uwindsor.ca (B. Zhou).

0378-7753/$ – see front matter © 2005 Elsevier B.V. All rights reserved.
doi:10.1016/j.jpowsour.2005.01.030

Nomenclature

a	water activity
A	area (m^2)
c	water concentration in the membrane ($mol\,m^{-3}$)
C_p	average heat capacity ($J\,kg^{-1}\,K^{-1}$)
d	channel height (m)
D_m	water diffusion coefficient ($m^2\,s^{-1}$)
E	thermodynamic potential (V)
f	fraction coefficient of channel
F	Faraday's constant ($F = 96{,}485$)
h	convective heat transfer coefficient ($W\,m^{-2}\,K^{-1}$)
H	change in enthalpy ($J\,mol^{-1}$)
ΔH	heat of reaction ($J\,mol^{-1}$)
i	operating current (A)
I	current density ($A\,cm^{-2}$)
I_0	exchange current density ($A\,cm^{-2}$)
k_p	water hydraulic permeability in membrane ($m^2\,s^{-1}$)
K	thermal conductivity ($W\,s^{-1}\,m^{-1}\,K^{-1}$)
L	channel length (m)
M	mass of the fuel cell (kg)
n	number of cells in the stack
n_d	electro-osmotic drag coefficient
n_e	mole number of electrons per unit current per unit time
N	molar flow rate ($mol\,s^{-1}$); channel number
P	power output (W)
PEM	proton exchange membrane
q	energy (W)
R	universal gas constant (=8.314 $J\,mol^{-1}\,K^{-1}$)
RH	relative humidity
t	thickness (m)
T	temperature (K)
V	output voltage (V); velocity ($m\,s^{-1}$)
x_i	mole fraction of species i

Greek letters

α	excess coefficient
η	over-voltage (V)
λ	water content of membrane
μ	water viscosity (Pa s)
ϕ	relative water content

Subscripts

0	standard condition
a	anode
act	activation
c	cathode
cell	proton exchange membrane fuel cell
cons	consumed
conv	convection flux
diff	diffusion flux
elec	electrical
g	gas
hum	humidification
in	in
inlet	flow inlet stack channel
int	internal
l	liquid
loss	loss
m	membrane
mass	mass transfer and/or mass consumption
ohmic	ohmic
out	out
outlet	flow outlet stack channel
prod	product
room	ambient condition
rxn	reaction
sens	sensible
stack	fuel cell stack
theo	theoretical
trans	water transfer across membrane
w	water

Superscripts

avg	average value
channel	stack flow channel
dry	dry gas condition
new	current value in iterative calculation
old	previous value in iterative calculation
sat	saturation condition
*	at the catalyst interface

The models mentioned above mainly emphasized on understanding and improving the kinetic processes that occurred in fuel cell, aiming at improving individual fuel cell performance. The researchers built their models based on electrochemical theories, electrode kinetics and experimental data.

As mentioned by Costamagna and Srinivasa [26], until the year 2000, no detailed results of the modeling analyses of the performance characteristics of the electrochemical cell stack and the PEMFC power plant had appeared in the literature. Models of fuel cell stacks have been and are being conducted by some fuel cell companies and such development remains in proprietary.

Texas A&M University [27,28] made very good contribution to the fuel cell stack modeling. However, their model only focused on fuel cell stack and the model did not consider two-phase flow and liquid water was not considered. In real fuel cell processes, both liquid water and vapor are very important factors that have to be resolved properly in order to have stable fuel cell operation.

Some thermal models of PEM fuel cell stacks could be found in the literature [29–32]. These models typically treat the stack as a process unit and develop models based on electrochemical performance, and the physical characteristics of the inlet and outlet flows. The computations of these models are usually too involved to be employed in a comprehensive model of a PEM fuel cell stack. A need exists for a technique that could be used to determine PEM fuel cell stack thermal performance without requiring significant amount of computations. Some excellent studies on these topics have been conducted by a group of scientists in Royal Military College of Canada [33–36]. In [37] by Yu and Zhou, an improved model was built to consider the inlet water vapor effects.

To the author's knowledge, the models mentioned above have not included the liquid water effects, especially the inlet water (liquid and vapor) effects that could play a very important role in the PEM fuel cell performance. Therefore, in the present study, a two-phase model with phase change was built to meet this challenge.

2. Model development

For modeling purposes, the following assumptions were made in the present study:

(1) The product water generated at the cathode is assumed to be in liquid state.
(2) The water condensation/evaporation rate is not considered. Instead, the equilibrium between the water vapor and liquid is always assumed.
(3) Ideal gas law was employed for gaseous species.
(4) Stack temperature is uniform due to high thermal conductivity.
(5) Water transport in and out of the electrodes was in the form of vapor.
(6) The electrode layers were "ultra-thin", so that gas transport resistance through the electrode porous layer could be neglected.
(7) The liquid water was assumed to exist at the surface of the channels, and the volume to be negligible.
(8) For the pressure drop calculation, the liquid water was neglected. The entrance and exit losses were neglected, which were too small compared with the overall pressure drop.

In order to describe both cases either with or without phase change, a parameter ϕ, relative water content, was defined as follows:

$$\phi = \frac{\text{Total mole number of water (vapor + liquid)}}{\text{Maximum possible mole number of water vapor}} \quad (1)$$

According to assumption (2), when $\phi \leq 1$, it is exactly the same as relative humidity and there is no liquid water; while $\phi > 1$ means there is liquid water and ϕ is no longer equivalent to the relative humidity.

2.1. Steady-state electrochemical model

The steady-state electrochemical model could be used to predict stack voltage output. The cell voltage was defined in terms of the following three terms [33]: the thermodynamic potential E, the activation over-voltage η_{act}, and the ohmic over-voltage η_{ohmic}:

$$V_{cell} = E - \eta_{act} - \eta_{ohmic} \quad (2)$$

where

$$E = 1.229 - 0.85 \times 10^{-3} \times (T_{stack} - 298.15) + 4.3085 \times 10^{-5} \times T_{stack} \times [\ln(p^*_{H_2}) + 0.5 \times \ln(p^*_{O_2})] \quad (3)$$

Here the friction effect (pressure drop) was introduced to modify the original model [33] by averaging the inlet and outlet partial pressures:

$$p^*_{H_2} = \tfrac{1}{2}(p^*_{H_2,in} + p^*_{H_2,out}) \quad (4)$$

$$p^*_{O_2} = \tfrac{1}{2}(p^*_{O_2,in} + p^*_{O_2,out}) \quad (5)$$

The activation overpotential and ohmic overpotential could be calculated as follows [19]:

$$\eta_{act} = \frac{R(273.15 + T_{stack})}{0.5F} \ln\left(\frac{I}{I_0 p_{O_2}}\right) \quad (6)$$

$$\eta_{ohmic} = \frac{I t_m}{\sigma_m} \quad (7)$$

where T_{stack} is the stack temperature (K), i the operating current (A), p^* the partial pressure on the catalyst interfaces corresponding to concentration of feeding gas, and I the current density.

2.2. Steady-state thermal model

A steady-state thermal model was established based on the balance of mass and energy about fuel cell stack. Fig. 1 shows a schematic of the inlet and outlet streams in a typical PEM fuel cell system. Hydrogen, air, and cooling water are independent streams. Energy balance about the fuel cell stack was performed to calculate various energy terms associated with fuel cell operation:

$$q_{theo} = q_{elec} + q_{sens} + q_{latent} + q_{loss} \quad (8)$$

where q_{theo} is the theoretical energy produced by the fuel cell reaction, q_{sens} the sensible heat calculated for each of the fuel cell streams (anode, cathode, and water coolant), q_{latent} the total latent heat of the water vaporization (condensation) for anode and cathode streams, q_{elec} the electrical energy output, and q_{loss} the heat loss from the surface of the stack. Comparing (8) with the model used in [33], the model developed in the present work included the two-phase effect (phase change).

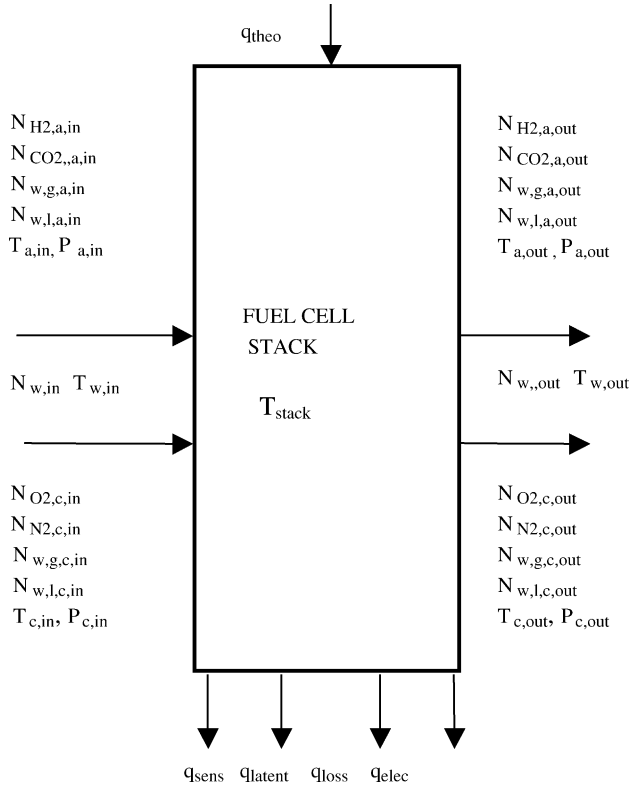

Fig. 1. Schematic of the inlet and outlet streams in a fuel cell system identifying various parameters including flow rates and energy terms.

2.2.1. Energy equations

Theoretical energy from the electrochemical reaction in PEM fuel cell was calculated through the product of reaction energy and molar flow rate of consumed hydrogen:

$$q_{\text{theo}} = N_{\text{H}_2,\text{cons}} \Delta H_{\text{rxn}} \tag{9}$$

The electrical power generated by the PEM fuel cell stack with n single cells was evaluated as

$$q_{\text{elec}} = n V_{\text{cell}} i \tag{10}$$

The sensible heat through anode stream was considered for all the possible species in anode (i.e., water vapor, liquid water, carbon dioxide from reformate) as follows:

$$\begin{aligned} q_{\text{sens,a}} = {} & N_{\text{H}_2,\text{a,out}} C_{p,\text{H}_2,\text{g}} (T_{\text{a,out}} - T_0) \\ & + N_{\text{w,g,a,out}} C_{p,\text{H}_2\text{O,g}} (T_{\text{a,out}} - T_0) \\ & + N_{\text{CO}_2,\text{a,out}} C_{p,\text{CO}_2,\text{g}} (T_{\text{a,out}} - T_0) \\ & + N_{\text{w,l,a,out}} C_{p,\text{w,l,out}} (T_{\text{a,out}} - T_0) \\ & - N_{\text{w,l,a,in}} C_{p,\text{w,l,in}} (T_{\text{a,in}} - T_0) \\ & - N_{\text{w,g,a,in}} C_{p,\text{H}_2\text{O,g}} (T_{\text{a,in}} - T_0) \\ & - N_{\text{H}_2,\text{a,in}} C_{p,\text{H}_2,\text{g}} (T_{\text{a,in}} - T_0) \\ & - N_{\text{CO}_2,\text{a,in}} C_{p,\text{CO}_2,\text{g}} (T_{\text{a,in}} - T_0) \end{aligned} \tag{11}$$

The latent heat through the anode was included through tracking down the phase change (in the present paper, the water vapor and water liquid were assumed to be in equilibrium all the time, i.e., the condensation/evaporation process was assumed to be so fast that there is no finite condensation/evaporation rate; also the water transfer across the membrane was assumed in vapor form, see details for this assumption in [19]):

$$q_{\text{latent,a}} = (N_{\text{w,g,a,out}} - N_{\text{w,g,a,in}} + N_{\text{trans}}) H_{\text{vaporization,a}} \tag{12}$$

The sensible heat in cathode was considered in a similar way to that in anode except the species are different from those in anode. In cathode the species include oxygen, nitrogen, water vapor, water liquid, as shown in (13):

$$\begin{aligned} q_{\text{sens,c}} = {} & N_{\text{O}_2,\text{c,out}} C_{p,\text{O}_2,\text{g}} (T_{\text{c,out}} - T_0) \\ & + N_{\text{w,g,c,out}} C_{p,\text{H}_2\text{O,g}} (T_{\text{c,out}} - T_0) \\ & + N_{\text{N}_2,\text{c,out}} C_{p,\text{N}_2,\text{g}} (T_{\text{c,out}} - T_0) \\ & + N_{\text{w,l,c,out}} C_{p,\text{w,l,out}} (T_{\text{c,out}} - T_0) \\ & - N_{\text{w,l,c,in}} C_{p,\text{w,l,in}} (T_{\text{c,in}} - T_0) \\ & - N_{\text{w,g,c,in}} C_{p,\text{H}_2\text{O,g}} (T_{\text{c,in}} - T_0) \\ & - N_{\text{O}_2,\text{c,in}} C_{p,\text{O}_2,\text{g}} (T_{\text{c,in}} - T_0) \\ & - N_{\text{N}_2,\text{c,in}} C_{\text{p,N}_2,\text{g}} (T_{\text{c,in}} - T_0) \end{aligned} \tag{13}$$

The latent heat in cathode is somehow complicated due to the water generation, water phase change and transfer across the membrane. The basic rule here is to figure out the molar flow rate of the water vapor that is involved in phase change. Details are as follows.

For latent heat in cathode, if $N_{\text{w,l,c,in}} \geq (N_{\text{w,g,c,out}} - N_{\text{trans}} - N_{\text{w,g,c,in}})$, i.e., the amount of liquid water carried from the cathode inlet is big enough for phase change, then we have

$$q_{\text{latent,c}} = (N_{\text{w,g,c,out}} - N_{\text{trans}} - N_{\text{w,g,c,in}}) H_{\text{vaporization1,c1}} \tag{14}$$

Otherwise, the liquid water carried from the inlet must be evaporated and some of product water must be evaporated too, so we have

$$\begin{aligned} q_{\text{latent,c}} = {} & N_{\text{w,l,c,in}} H_{\text{vaporization,c1}} + (N_{\text{w,g,c,out}} - N_{\text{trans}} \\ & - N_{\text{w,g,c,in}} - N_{\text{w,l,c,in}}) H_{\text{vaporization,c2}} \end{aligned} \tag{15}$$

where

$$\begin{aligned} H_{\text{vaporization}} = {} & 45070 - 41.9T + 3.44 \times 10^{-3} T^2 \\ & + 2.54 \times 10^{-6} T^3 - 8.98 \times 10^{-10} T^4 \end{aligned} \tag{16}$$

and subscripts c1 and c2 represent the different state (thus different temperature) for the evaporation of water that are from different origin, e.g., either from inlet stream or electrochemical product.The sensible heat in water coolant stream was calculated by use of the following formula:

$$q_{\text{sens,w}} = N_{\text{w,in}} C_{p,\text{w,l}}(T_{\text{w,out}} - T_0) - N_{\text{w,in}} C_{p,\text{w,l}}(T_{\text{w,in}} - T_0) \quad (17)$$

Then the sensible and latent heat were summed and the heat loss from the stack to the ambient was calculated based on (8):

$$q_{\text{sens}} = q_{\text{sens,a}} + q_{\text{sens,c}} + q_{\text{sens,w}} \quad (18)$$

$$q_{\text{latent}} = q_{\text{latent,a}} + q_{\text{latent,c}} \quad (19)$$

$$q_{\text{loss}} = q_{\text{theo}} - q_{\text{elec}} - q_{\text{sens}} - q_{\text{latent}} \quad (20)$$

2.2.2. Flow rates

The saturation pressure (atm) was calculated based on the following equation [19]:

$$p^{\text{sat}}_{\text{w,g}} = 10^{-2.1794+0.02953T-9.1837\times10^{-5}T^2+1.4454\times10^{-7}T^3} \quad (21)$$

The molar flow rate for hydrogen in anode and air in cathode on dry condition at each inlet can be evaluated according to the operating current and excess coefficient [37] on each stream inlet:

$$N_{\text{a,H}_2\text{,in,dry,0}} = \frac{1}{2\beta_{\text{H}_2}} I\alpha_{\text{H}_2} n_{\text{e}} \quad (22)$$

$$N_{\text{c,air,in,dry,0}} = \frac{1}{4\beta_{\text{O}_2}} I\alpha_{\text{O}_2} n_{\text{e}} \quad (23)$$

where $n_{\text{e}} = 1.0365 \times 10^{-5}$ mol/A s is the molar flow rate of electrons for generating 1 A electricity, α the excess coefficient, i.e., the ratio of the actual amount supplied to the theoretical amount needed, and β the molar fraction of oxygen in air stream at cathode inlet.

The equations of flow rates were proposed to account for the inlet water (liquid + vapor), as listed below.

The maximum water vapor carried from the anode inlet was evaluated as

$$N_{\text{w,g,a,in,max}} = (N_{\text{H}_2\text{,a,in}} + N_{\text{CO}_2\text{,a,in}}) \frac{p^{\text{sat}}_{\text{w,g,a,in}}}{p_{\text{a,in}} - p^{\text{sat}}_{\text{w,g,a,in}}} \quad (24)$$

Then the amount of water vapor and water liquid at the anode inlet were calculated as below.

If $N_{\text{w,a,in}} \geq N_{\text{w,g,a,in,max}}$, then we have

$$N_{\text{w,g,a,in}} = N_{\text{w,g,a,in,max}},$$
$$N_{\text{w,l,a,in}} = N_{\text{w,a,in}} - N_{\text{w,g,a,in}} \quad (25)$$

If $N_{\text{w,a,in}} < N_{\text{w,g,a,in,max}}$, then we have

$$N_{\text{w,g,a,in}} = (N_{\text{H}_2\text{,a,in}} + N_{\text{CO}_2\text{,a,in}}) \frac{p^{\text{sat}}_{\text{w,g,a,in}} \phi_{\text{a,in}}}{p_{\text{a,in}} - p^{\text{sat}}_{\text{w,g,a,in}} \phi_{\text{a,in}}},$$
$$N_{\text{w,l,a,in}} = 0 \quad (26)$$

The maximum amount of water vapor at anode outlet was calculated as follows:

$$N_{\text{w,g,a,out,max}} = (N_{\text{H}_2\text{,a,out}} + N_{\text{CO}_2\text{,a,out}}) \frac{p^{\text{sat}}_{\text{w,g,a,out}}}{p_{\text{a,out}} - p^{\text{sat}}_{\text{w,g,a,out}}} \quad (27)$$

Then the amount of water vapor and water liquid in the anode outlet were evaluated as below.

If $N_{\text{w,a,in}} - N_{\text{trans}} \geq N_{\text{w,g,a,out,max}}$, then we have

$$N_{\text{w,g,a,out}} = N_{\text{w,g,a,out,max}},$$
$$N_{\text{w,l,a,out}} = N_{\text{w,a,in}} - N_{\text{trans}} - N_{\text{w,g,a,out}} \quad (28)$$

If $N_{\text{w,a,in}} - N_{\text{trans}} < N_{\text{w,g,a,out,max}}$, then we have

$$N_{\text{w,g,a,out}} = N_{\text{w,a,in}} - N_{\text{trans}}, \qquad N_{\text{w,l,a,out}} = 0 \quad (29)$$

For cathode inlet, the maximum water vapor carried from the cathode inlet was evaluated as

$$N_{\text{w,g,c,in,max}} = (N_{\text{O}_2\text{,c,in}} + N_{\text{N}_2\text{,c,in}}) \frac{p^{\text{sat}}_{\text{w,g,c,in}}}{p_{\text{c,in}} - p^{\text{sat}}_{\text{w,g,c,in}}} \quad (30)$$

Then the amount of water vapor and water liquid in the cathode inlet were evaluated as below.

If $N_{\text{w,c,in}} \geq N_{\text{w,g,c,in,max}}$, then we have

$$N_{\text{w,g,c,in}} = N_{\text{w,g,c,in,max}},$$
$$N_{\text{w,l,c,in}} = N_{\text{w,c,in}} - N_{\text{w,g,c,in}} \quad (31)$$

If $N_{\text{w,c,in}} < N_{\text{w,g,c,in,max}}$, then we have

$$N_{\text{w,g,c,in}} = (N_{\text{O}_2\text{,c,in}} + N_{\text{N}_2\text{,c,in}}) \frac{p^{\text{sat}}_{\text{w,g,c,in}} \phi_{\text{c,in}}}{p_{\text{c,in}} - p^{\text{sat}}_{\text{w,g,c,in}} \phi_{\text{c,in}}},$$
$$N_{\text{w,l,c,in}} = 0 \quad (32)$$

In cathode stream, the water was produced and the product water was assumed to be liquid in the present study. It was evaluated as

$$N_{\text{w,l,prod}} = N_{\text{H}_2\text{,cons}} = N_{\text{H}_2\text{,a,in}} - N_{\text{H}_2\text{,a,out}} \quad (33)$$

For cathode outlet, the maximum water vapor carried from the cathode outlet was evaluated as

$$N_{\text{w,g,c,out,max}} = (N_{\text{O}_2\text{,c,out}} + N_{\text{N}_2\text{,c,out}}) \frac{p^{\text{sat}}_{\text{w,g,c,out}}}{p_{\text{c,out}} - p^{\text{sat}}_{\text{w,g,c,out}}} \quad (34)$$

Then the amount of water vapor and water liquid in the cathode outlet were evaluated as below.

If $(N_{\text{w,c,in}} + N_{\text{w,l,prod}} + N_{\text{trans}}) \geq N_{\text{w,g,c,out,max}}$, then we have

$$N_{\text{w,g,c,out}} = N_{\text{w,g,c,out,max}},$$
$$N_{\text{w,l,c,out}} = N_{\text{w,c,in}} + N_{\text{w,l,prod}} + N_{\text{trans}} - N_{\text{w,g,c,out}} \quad (35)$$

If $(N_{\text{w,c,in}} + N_{\text{w,l,prod}} + N_{\text{trans}}) < N_{\text{w,g,c,out,max}}$, then we have

$$N_{w,g,c,out} = N_{w,c,in} + N_{w,l,prod} + N_{trans},$$
$$N_{w,l,c,out} = 0 \quad (36)$$

The average heat transfer coefficient for the stack may be estimated using the average heat loss from the surface of the fuel cell stack. Similarly, the increase in sensible and latent heat terms could also be linked to heat transfer coefficients, h_j, from the stack to the fluid j, where j = anode, cathode, or water stream. Once heat transfer coefficients h, heat exchange area and sensible, latent heat terms are known, the temperature of stack and outlet flows could be estimated by using the following equations:

$$T_{stack} = \frac{q_{loss}}{(hA)_{stack}} + T_{room} \quad (37)$$

$$T_{a,out} = 2\left[T_{stack} - \frac{q_{sen,a} + q_{latent,a} + q_{mass,a}}{(hA)_a}\right] - T_{a,in} \quad (38)$$

$$T_{c,out} = 2\left[T_{stack} - \frac{q_{sen,c} + q_{latent,a} - q_{mass,c}}{(hA)_c}\right] - T_{c,in} \quad (39)$$

$$T_{w,out} = 2\left[T_{stack} - \frac{q_{sen,w}}{(hA)_w}\right] - T_{w,in} \quad (40)$$

where the energy change due to mass transfer and mass consumption (including the sensible energy carried by the water transfer across the membrane, the sensible energy carried by hydrogen/oxygen consumed) was evaluated as follows:

$$q_{mass,a} = N_{trans}C_{p,H_2O,g}(T_{stack} - T_0) + N_{H_2,con}C_{p,H_2,g}(T_{stack} - T_0) \quad (41)$$

$$q_{mass,c} = N_{trans}C_{p,H_2O,g}(T_{stack} - T_0) + N_{H_2,con}C_{p,H_2O,l}(T_{stack} - T_0) - N_{O_2,con}C_{p,O_2}(T_{stack} - T_0) \quad (42)$$

2.3. Transient model

In transient state, an additional accumulation term should be considered, therefore:

$$m_{stack}C_{p,stack}\frac{dT_{stack}}{dt} = q_{theo} - q_{elec} - q_{sens} - q_{latent} - q_{loss} \quad (43)$$

where m is the total mass of the fuel cell stack, C the average specific heat of the stack, and dT_{stack}/dt the temperature change with respect to time. From Eq. (43), we have

$$\frac{dT_{stack}}{dt} = \frac{q_{theo} - q_{elec} - q_{sens} - q_{latent} - q_{loss}}{m_{stack}C_{p,stack}} \quad (44)$$

In the calculations presented, an average value of 35 kJ K^{-1} was used for $m_{stack}C_{p,stack}$ of Ballard Mark V stack. Knowing all the terms on the right side of the Eq. (44), it could be used as a basis of a finite-difference calculation using

$$T_{stack}^{new} = T_{stack}^{old} + \frac{dT_{stack}}{dt}\Delta t \quad (45)$$

2.4. Pressure drop

Pressure drop along the channels could be calculated by using average gas velocity, which is the mean value of inlet and outlet velocity of each stream. Ignoring the volume of liquid water, the local velocity V (m s^{-1}) was determined by gas molar flow rate (mol s^{-1}), local pressure, temperature, cross-section area of channel A_c, and number of channels (N_{ch}):

$$V = \frac{N \times 22.4 \times 10^{-3}}{A_c N_{ch}}\frac{p_0}{p}\frac{T}{T_0} \quad (46)$$

where the gas molar flow rate could be determined for each stream as follows.

at anode inlet:

$$N = (N_{H_2,a,in} + N_{CO_2,a,in})\left(1 + \frac{p_{w,g,a,in}^{sat}\,RH_{a,in}}{p_{a,in} - p_{w,g,a,in}^{sat}\,RH_{a,in}}\right) \quad (47)$$

at anode outlet:

$$N = (N_{H_2,a,out} + N_{CO_2,a,out}) \times \left(1 + \frac{p_{w,g,a,out}^{sat}\,RH_{a,out}}{p_{a,out} - p_{w,g,a,out}^{sat}\,RH_{a,out}}\right) \quad (48)$$

at cathode inlet:

$$N = (N_{O_2,c,in} + N_{N_2,c,in})\left(1 + \frac{p_{w,g,c,in}^{sat}\,RH_{c,in}}{p_{c,in} - p_{w,g,c,in}^{sat}\,RH_{c,in}}\right) \quad (49)$$

at cathode outlet:

$$N = (N_{O_2,c,out} + N_{N_2,c,out}) \times \left(1 + \frac{p_{w,g,c,out}^{sat}\,RH_{c,out}}{p_{c,out} - p_{w,g,c,out}^{sat}\,RH_{c,out}}\right) \quad (50)$$

When RH = 1, the largest molar flow rate for each stream is obtained.Once temperature and flow rate are known, the pressure drop along the channels could be obtained by using (Darcy-Weisbach equation [38]):

$$\Delta p_a = f_a \times \frac{L_a}{D_a}\frac{\rho_a V_{a,m}^2}{2} \quad (51)$$

$$\Delta p_c = f_c \times \frac{L_c}{D_c}\frac{\rho_c V_{c,m}^2}{2} \quad (52)$$

where D is the hydraulic diameter.

2.5. Water transfer across membrane

Water transfer across membrane is the sum of following three terms [19,39]:

1. Electro-osmotic drag flux, which is caused by hydrogen ion drag.
2. Diffusion flux, which is caused by water concentration gradient between anode and cathode.
3. Convection flux, which caused by pressure gradient.

Therefore,

$$N_{\text{trans}} = N_{\text{drag}} + N_{\text{diff}} + N_{\text{conv}} \tag{53}$$

The electro-osmotic drag flux could be calculated by [19,39]:

$$N_{\text{drag}} = n_{\text{d}} \frac{I(x)}{F} \tag{54}$$

$$n_{\text{d}} = \frac{2.5}{22}\lambda \tag{55}$$

$$\begin{aligned}\lambda &= 0.043 + 17.81a - 39.85a^2 + 36.0a^3 \,\text{at}\, (a < 1) \\ &= 14.0 + 1.4(a-1)\, at\, (3 \geq a \geq 1) = 16.8 \,\text{at}\, (a \geq 3)\end{aligned} \tag{56}$$

$$a = \frac{p_{\text{vapor}}}{p_{\text{sat}}} \tag{57}$$

where n_{d} is called electro-osmotic drag coefficient, I the current density, a the water vapor activity (ratio of the water vapor pressure and the saturation pressure), λ the water content of membrane that is related with water vapor activity.Diffusion drag flux is decided by diffusion coefficient D_{m}, water concentration c and the membrane charge concentration c_{f} which is fixed for one type of membrane [19,39].

$$\begin{aligned}D_{\text{m}} &= 10^{-10} \exp\left[2416\left(\frac{1}{303}\right) - \left(\frac{1}{T}\right)\right](2.563 - 0.33\lambda \\ &\quad + 0.0264\lambda^2 - 0.000671\lambda^3) \,\text{at}\, (\lambda > 4) \\ &= 10^{-10} \exp\left[2416\left(\frac{1}{303}\right) - \left(\frac{1}{T}\right)\right](-1.25\lambda \\ &\quad + 6.65) \,\text{at}\, (4 \geq \lambda \geq 3) \\ &= 10^{-10} \exp\left[2416\left(\frac{1}{303}\right) - \left(\frac{1}{T}\right)\right](2.05\lambda \\ &\quad - 3.25) \,\text{at}\, (3 > \lambda \geq 2)\end{aligned} \tag{58}$$

$$c = \lambda c_{\text{f}} \tag{59}$$

$$N_{\text{diff,y}} = -D_{\text{m}} \frac{\text{d}c}{\text{d}y} = -D_{\text{m}} c_{\text{f}} \frac{\text{d}\lambda}{\text{d}y} \tag{60}$$

Convection flux was calculated as follows:

$$N_{\text{conv,y}} = -\frac{k_{\text{p}}}{\mu} c \frac{\text{d}p_{\text{v}}}{\text{d}y} = -\frac{k_{\text{p}}}{\mu} \lambda c_{\text{f}} \frac{\text{d}p_{\text{v}}}{\text{d}y} \tag{61}$$

where k_{p}, μ, $\text{d}p_{\text{v}}$ and c are the hydraulic permeability of water in membrane, water viscosity, partial pressure difference between anode and cathode, and concentration of water in membrane.

3. Solution methodology

3.1. Steady-state models

Step 1. Start with a guess or estimate for the values of T_{stack}, $T_{\text{w,out}}$, $T_{\text{a,out}}$, $T_{\text{c,out}}$ and p_{out}.
Step 2. From these guessed values, calculate tentative values of related energy terms and V_{cell}.
Step 3. Use those tentative energy values and heat transfer coefficients to get new values of T and p.
Step 4. With these p, T as better guesses, return to step 2, repeat the process until further repetitions cease producing any significant changes in these values.
Step 5. These final values of T, p will satisfy energy and mass balance, and will be the steady-state result of the stack.
Step 6. Other related values of parameter can be calculated from them.

3.2. Unsteady-state models

The time step $\Delta t = 1$ s was used in the dynamic calculations, thus changes of all the parameters could be traced at each second.

Step 1. Calculate energy term and V_{cell} by initial input values. Use unsteady-state thermal model equation to get the value of $\text{d}T_{\text{stack}}/\text{d}t$ at the beginning of the first time step.
Step 2. Calculate T_{stack} value at the end of the first time step, guess the value of $T_{\text{w,out}}$, $T_{\text{a,out}}$, $T_{\text{c,out}}$ and p_{out}.
Step 3. Keep fixed value of T_{stack}, follow steady-state calculation steps to find all parameter values at the end of the first time step.
Step 4. For next time step, go to step 1, use those value got from step 3 as the initial values, and repeat the process until reach the end of time period.

4. Results and discussions

4.1. Steady cases

In the calculations presented here, unless specified otherwise, RH = 1 for both anode and cathode inlet stream. Table 1 shows the input data for the calculated case that was similar to the case reported by Amphlett et al. [36] and a comparison has been discussed by Yu and Zhou [37].

Table 1
Input data for calculated case (I = 20 A)

Parameter	Value
$N_{H_2,a,in}$ (mol s^{-1})	0.0078
$T_{a,in}$ (°C)	23.5
$P_{a,in}$ (psig)	35
$N_{O_2,c,in}$ (mol s^{-1})	0.004
$T_{c,in}$ (°C)	23.5
$P_{c,in}$ (psig)	35
$N_{w,in}$ (mol s^{-1})	1.84
$T_{w,in}$ (°C)	23.5
T_{room} (°C)	23.5
k_{cell}	35 cells

Fig. 2 shows temperature of the exits at anode, cathode, and water coolant with respect to the steady operating currents from 1 to 60 A. It could be seen that all the temperatures increased with the increase of steady operating current and the cathode exit temperature was higher than the stack temperature, anode temperature and coolant temperature.

Fig. 3 is the output stack power at different steady operating currents from 1 to 60 A. The power output almost increased linearly with the steady operating current.

4.2. Steady cases with different values of ϕ at inlets

In Fig. 4, the anode exit temperature at $\phi_{a,in}$ = 1.0 and 1.5 was plotted. Here $\phi_{a,in}$, relative water content at anode inlet, represents the molar ratio between total amount of supplied water (liquid + vapor) at anode inlet and the saturated water vapor carried by the anode inlet stream. When $\phi_{a,in} < 1$, the anode outlet temperature did not vary significantly with $\phi_{a,in}$ (Fig. 4a). When $\phi_{a,in} > 1$, liquid water would mix with anode inlet stream and thus different $\phi_{a,in}$ values would have an obvious effect on anode outlet temperature, attributable to liquid water vaporization leading to anode exit temperature reduc-

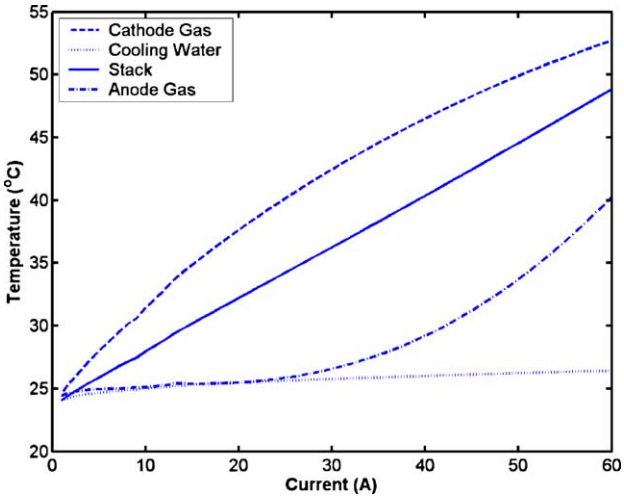

Fig. 2. Stack temperature and exit temperatures at anode, cathode, and water coolant with steady operating currents from 1 to 60 A.

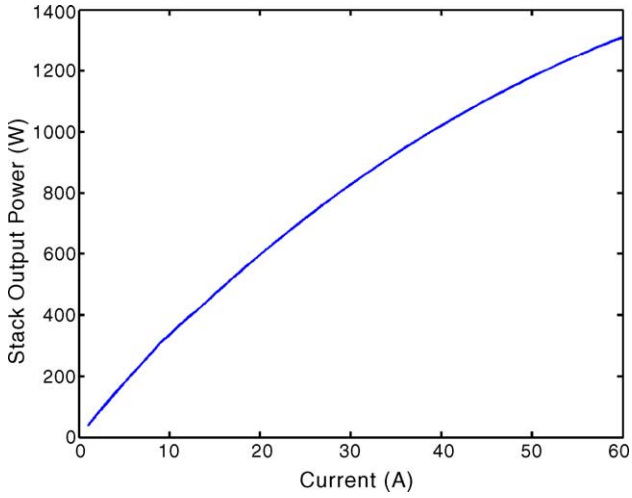

Fig. 3. Stack output power with steady operating current from 1 to 60 A.

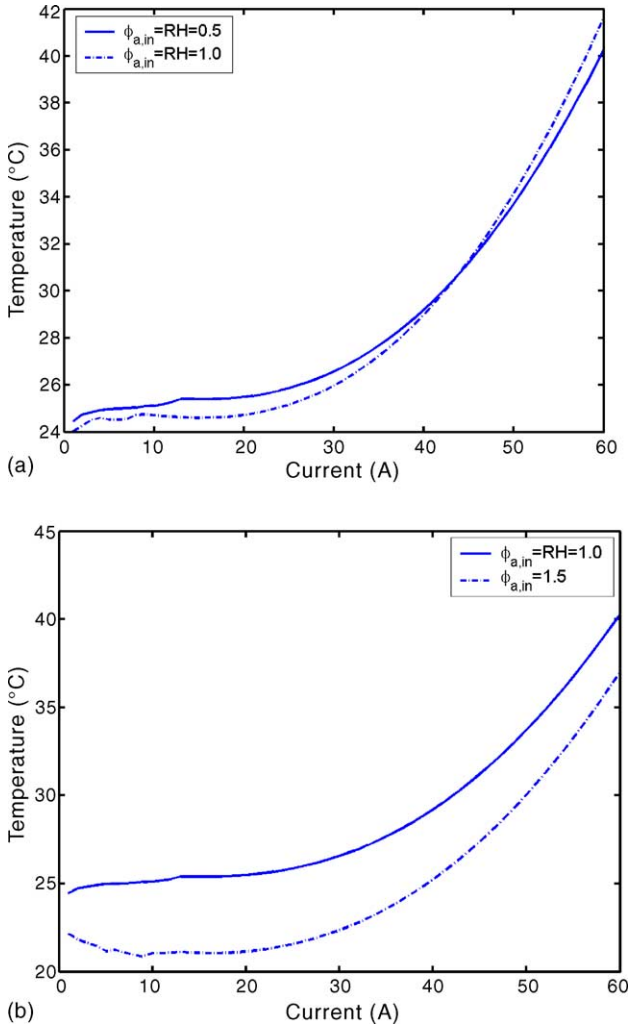

Fig. 4. (a) Anode exit temperature at $\phi_{a,in}$ = 0.5 and 1.0. (b) Anode exit temperature at different $\phi_{a,in}$ value 1.0 and 1.5.

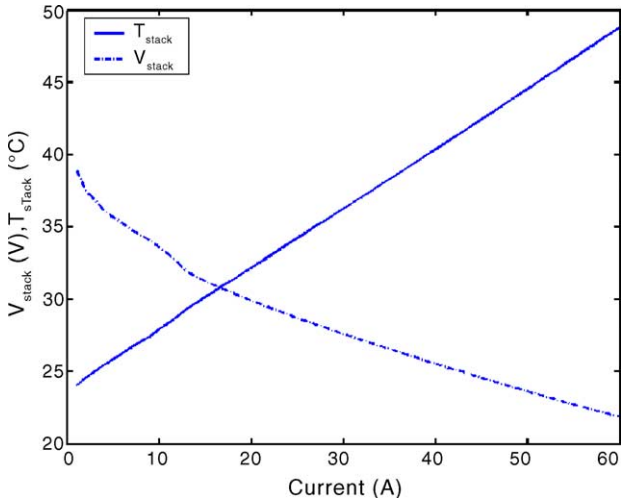

Fig. 5. Stack temperature and voltage with different steady operating current from 1 to 60 A.

tion (Fig. 4b). Basically, when inlet $\phi_{a,in}$ value increased, the anode exit temperature decreased.

Fig. 5 shows the stack temperature and voltage with different operating currents. Output voltage decreased when current was increased, attributable to a higher current creating a larger ohmic over-voltage loss. Fig. 6 shows stack voltage output at different $\phi_{a,in}$ for steady operating conditions. Electro-osmotic drag would be the dominant factor affecting the amount of water transferred across the membrane. Water was dragged from the anode to cathode side resulting in dry gas at the anode side which would reduce membrane conductivity and subsequently lower the stack voltage. Therefore, in order to achieve a higher voltage output, extra humidification has to be provided to the gas at the anode side; It also could be seen in Fig. 6 that voltage output increased when the inlet $\phi_{a,in}$ was raised.

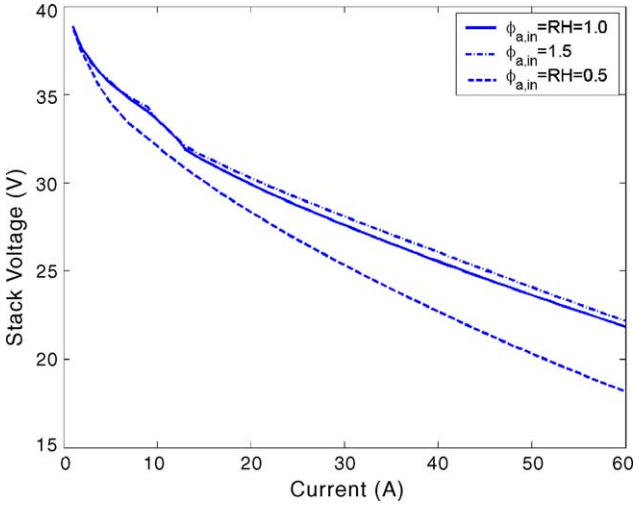

Fig. 6. Stack voltage with different $\phi_{a,in}$ at steady operating current from 1 to 60 A.

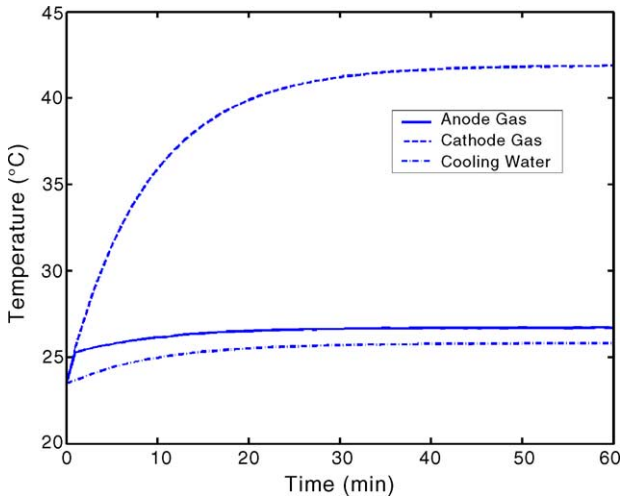

Fig. 7. Transient exit temperature plots of the start-up process for the operating current at 30 A.

4.3. Unsteady cases

Figs. 7 and 8 show the start-up characteristics of this stack at the operating current of 30 A; Fig. 7 shows the transient exit temperature plots while Fig. 8 shows the stack temperature and voltage.

From Figs. 7 and 8, it could be seen that the stack required about 30–40 min to reach steady state with the operating current of 30 A. In the first 20 min, the rate-of-exit temperature increase was high then slowly reduced until about 40 min when the stack almost reached its steady operating state.

The transient response of the stack for the load-set-up from 30 A (for 60 min) to 50 A (for another 60 min) are shown in Figs. 9 and 10. In general, the stack required about 40 min to reach its steady operating state after the load was changed. It is noteworthy that when the load was changed from 30 to 50 A, the immediate exit temperatures of cathode and water

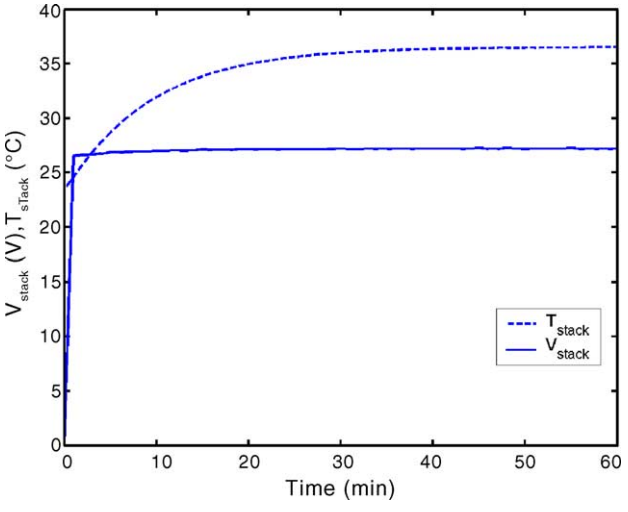

Fig. 8. Transient plot for the stack temperature and voltage of the start-up process for the operating current at 30 A.

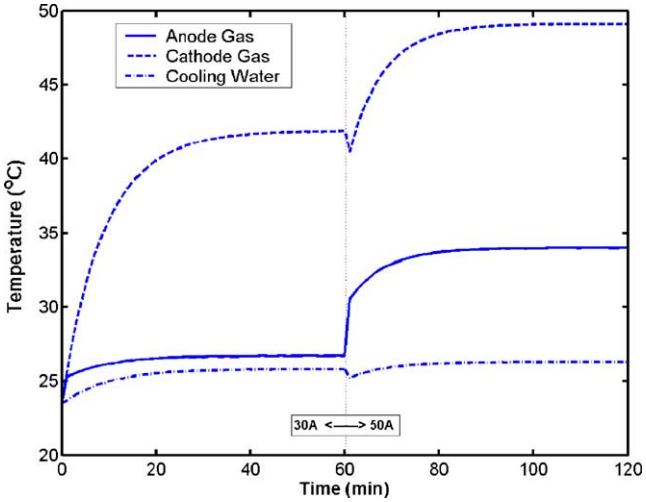

Fig. 9. Transient plot of exit temperatures at anode, cathode and water coolant during the load set-up from 30 to 50 A.

coolant decreased because the amount of air and water with lower temperature increased from the inlets. Furthermore, from Fig. 10, the stack voltage at operating current of 50 A was lower than that at 30 A, due to the increase of current that would create larger over-voltages and thus smaller cell and stack voltage.

Fig. 11 shows the temperature change in all streams as function of time and current change while Fig. 12 gives the stack voltage output and temperature change as function of time and load change. The load changed in each 20 min, from 20 to 40, to 60, to 40, and to 20 A within 100 min.

Fig. 13 shows the values of stack voltage in terms of current change as a sine function $I = 31+30\sin(t\pi/30)$ where the stack current curve was plotted as a reference. During the current change from 1 to 61 A, the voltage output slew in the range 27–38 V and the minimum voltage output value was attained when the current (power output curve had the

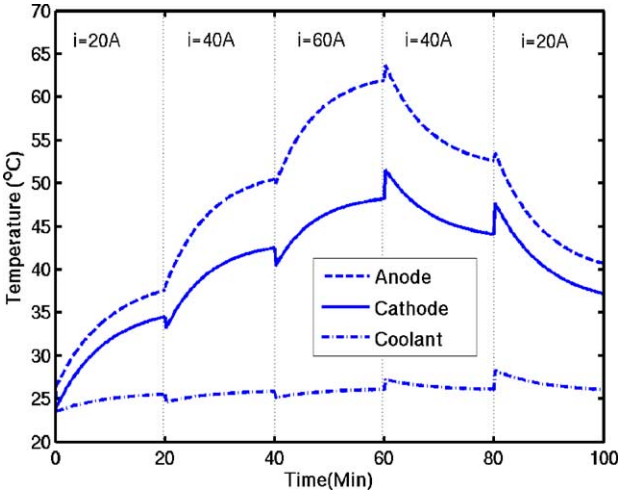

Fig. 11. Exit temperature change with time/load ($\phi_{a,in} = \phi_{c,in} = 1.0$).

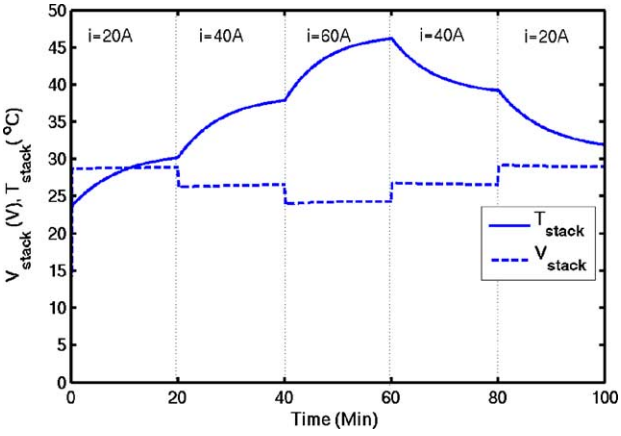

Fig. 12. Stack temperature and voltage change ($\phi_{a,in} = \phi_{c,in} = 1.0$).

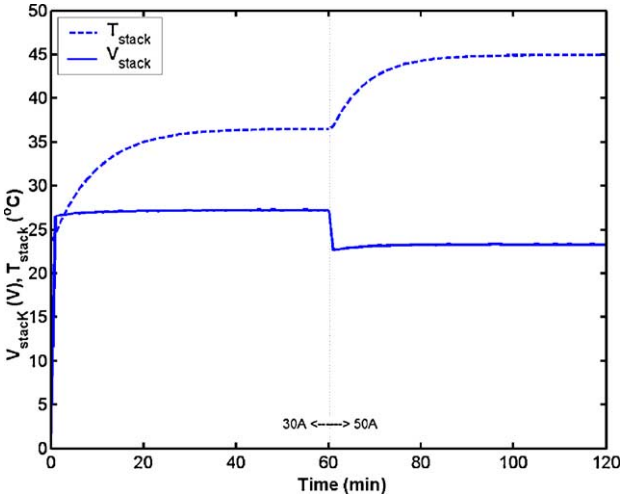

Fig. 10. Transient plot of stack temperature and voltage during the load set-up from 30 to 50 A.

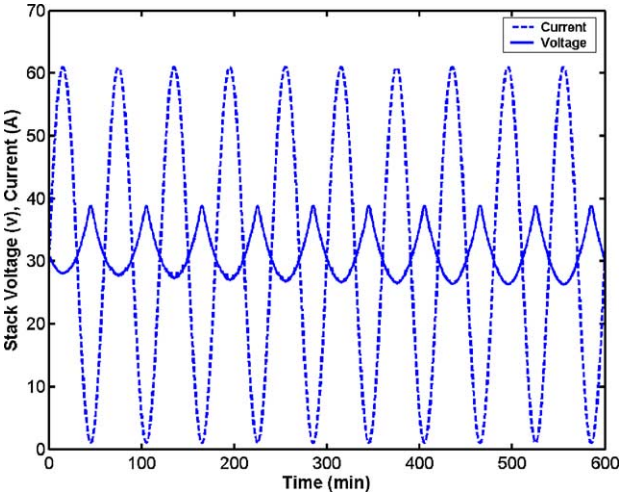

Fig. 13. Stack voltage as a function of current which changes with time as $I = 31 + 30\sin(t\pi/30)$.

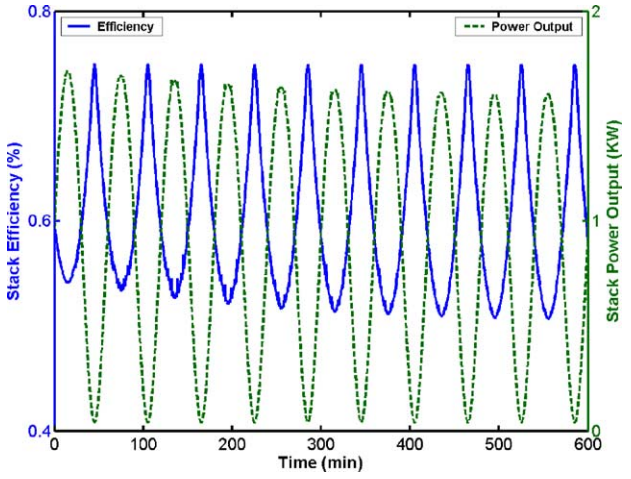

Fig. 14. Stack efficiency and power as a function of current which changes with time as $I = 31+30\sin(t\pi/30)$.

same pace) was at its maximum value due to voltage ohmic loss.

For the steady case, the average efficiency was around 45–65%, depending on the voltage, energy loss to the surrounding and the stream sensible heat. For the unsteady case, when the current approached zero, the efficiency approached its peak value with the maximum attained at close to 0 A; the efficiency then quickly reduced as the current increased as observed in Fig. 14. When the current and power output had the same phase, therefore, when the current reached its peak in each period, the power output also reached its maximum value, however, stack efficiency had the opposite trend (Figs. 13 and 14).

5. Conclusions

The main objective of the present study was to investigate the Ballard PEM fuel cell performance in terms of electrochemical characteristics, and thermal and water management. A simplified mathematical model and tool, which could be used to evaluate PEM fuel cell stack electrochemical performance as well as water and thermal management, has been proposed and implemented to simulate a Ballard PEM fuel cell stack.

The model and tool can be applied in PEM fuel call design processes to assist the designer in achieving an optimal design. Knowing a set of gas feeding and stack physical conditions, the design engineer can obtain the information regarding reaction products, stack power, temperature, system efficiency, and dynamic characteristic of the PEM fuel cell stack, by use of the numerical trial-and-error method developed in the present study.

For the studied Ballard PEM fuel cell stack, the more the water supplied to anode from its inlet ($\phi_{a,in} = 1.0$ and 1.5), the higher the voltage, and usually the lower the anode exit temperature. The studied Ballard PEM fuel cell stack usually takes about 30–40 min to reach its steady operation.

Acknowledgement

This work was supported in part by the Auto21 Networks of Centres of Excellence Grant D07-DFC.

References

[1] J. Larminie, A. Dicks, Fuel Cell Systems Explained, Wiley, 2002.
[2] T. Yokoyama, Y. Naganuma, K. Kuriyama, M. Arimoto, Development of fuel-cell bus, SAE Paper 1 (2003) 4–17.
[3] J.K. Seong, O.B. Soo, Fuel economy and life-cycle cost analysis of a fuel cell hybrid vehicle, J. Power Sources 105 (2002) 58–65.
[4] M. Ogburn, D.J. Nelson, W. Luttrell, B. King, S. Postle, R. Fahrenkrog, Systems integration and performance issues in a fuel cell hybrid electric vehicle, SAE Pap. 1 (2000) 3–76.
[5] J.M. Ogden, M.M. Steinnbugler, T.G. Kreutz, A comparison of hydrogen, methanol and gasoline as fuels for fuel cell vehicles: implications for vehicle design and infrastructure development, J. Power Sources 79 (2) (1999) 143–168.
[6] E. Per, R. Monika, The fuel cell vehicle analysis of energy use, emissions and cost, Int. J. Hydrogen Energy 23 (5) (1998) 381–385.
[7] Y.J. Zhang, M.G. Ouyang, J.X. Luo, Z. Zhang, Y.J. Wang, Mathematical modeling of vehicle fuel cell power system thermal management, SAE Pap. 1 (2003) 11–46.
[8] R. Andrew, X.G. Li, Mathematical modeling of proton exchange membrane fuel cells, J. Power Sources 102 (2001) 82–96.
[9] Transportation Fuel Cell Power Systems Annual Progress Report, US. Department of Energy, December 2001.
[10] Transportation Fuel Cell Power Systems Annual Progress Report, US. Department of Energy, October 2000.
[11] M. Nadal, F. Barbir, Development of a hybrid fuel cell/battery powered electric vehicle, Int. J. Hydrogen Energy 21 (1996) 497–505.
[12] J.C. Amphlett, R.M. Baumert, R.F. Mann, B.A. Peppley, P.R. Roberge, Parametric modeling of the performance of a 5-kW proton exchange membrane fuel cell stack, J. Power Sources 49 (1994) 349–356.
[13] W.R. Dunbar, R.A. Gaggioli, Computer simulation of solid electrolyte fuel cells, J. Energy Resources Technol. 112 (1990) 1–14.
[14] T.E. Apringer, T.A. Zawodzinski, S. Gottesfeld, Polymer electrolyte fuel cello model, J. Electrochem. Soc. 138 (8) (1991) 2334–2342.
[15] M.W. Verbrugge, R.F. Hill, Transport phenomena in perfluorosulfonic acid membranes during the passage of current, J. Electrochem. Soc. 137 (4) (1990) 1131–1138.
[16] D.M. Bernardi, M.W. Verbrugge, Mathematical model of a gas diffusion electrode bonded to a polymer electrolyte, AICHE J. 37 (8) (1991) 1151–1163.
[17] D.M. Bernardi, M.W. Verbrugge, A mathematical model of the solid–polymer–electrolyte fuel cell, J. Electrochem. Soc. 139 (9) (1992) 2477–2491.
[18] T.F. Fuller, J. Newman, Water and thermal management in solid–polymer–electrolyte fuel cells, J. Electrochem. Soc. 140 (5) (1993) 1218–1225.
[19] T.V. Nguyen, R.E. White, A water and heat management model for proton-exchange-membrane fuel cells, J. Electrochem. Soc. 140 (8) (1993) 2178–2186.
[20] J. Kim, S. Srinivasan, C.E. Chamberlin, Modeling of proton exchange membrane fuel cell performance with an empirical equation, J. Electrochem. Soc. 142 (8) (1993) 2670.

[21] T. Berning, D.M. Lu, N. Djilali, Three-dimensional analysis of transport phenomena in a PEM fuel cell, J. Power Sources 106 (2002) 284–294.
[22] A. Rowe, X. Li, Mathematical modeling of proton exchange membrane fuel cells, J. Power Sources 102 (2001) 82–96.
[23] J.J. Baschuk, X. Li, Modeling of polymer electrolyte membrane fuel cells with variable degrees of water flooding, J. Power Sources 86 (2000) 181–196.
[24] C. Marr, X. Li, Composition and performance modeling of catalyst layer in a proton exchange membrane fuel cell, J. Power Sources 77 (1999) 17–27.
[25] D. Xue, Z. Dong, Optimal fuel cell system design considering functional performance and production costs, J. Power Sources 76 (1998) 69–80.
[26] P. Costamagna, S. Srinivasa, Quantum jumps in the PEMFC science and technology from the 1960s to the year 2000. Part II. Engineering, technology development and application aspects, J. Power Sources 102 (2001) 253–269.
[27] J.H. Lee, T.R. Lark, A.J. Appleby, Modeling electrochemical performance in large scale proton exchange membrane fuel cell stacks, J. Power Sources 70 (1998) 258–268.
[28] J.H. Lee, T.R. Lark, Modeling fuel cell stack systems, J. Power Sources 73 (1998) 229–241.
[29] N. Djilali, D.M. Lu, Influence of heat transfer on gas and water transport in fuel cells, Int. J. Therm. Sci. 41 (2002) 29–40.
[30] N.S. Ap, Influence of front end vehicle, fan and fan shroud on the cooling system of fuel cell electric vehicle (FCEV), EVS 18, Berlin, 2001.
[31] M.H. Fronk, D.L. Wetter, D.A. Masten, A. Bosco, PEM fuel cell system solutions for transportation, SAE Pap. 1 (2000) 373.
[32] G. Maggio, V. Recupero, C. Mantegazza, Modeling of temperature distribution in a solid polymer electrolyte fuel cell stack, J. Power Sources 62 (1996) 167–174.
[33] J.C. Amphlett, R.M. Baumert, R.F. Mann, B.A. Peppley, P.R. Roberge, A. Rodrigues, Parametric modelling of the performance of a 5-kW proton exchange membrane fuel cell stack, J. Power Sources 49 (1994) 349–356.
[34] J.C. Amphlett, R.M. Baumert, R.F. Mann, B.A. Peppley, P.R. Roberge, T.J. Harris, Performance modeling of the Ballard Mark IV solid polymer electrolyte fuel cell: II empirical model development, J. Electrochem. Soc. 142 (1995) 9–15.
[35] J.C. Amphlett, R.M. Naumert, R.F. Mann, B.A. Peppley, P.R. Roberge, T.J. Harris, Performance modeling of the Ballard Mark IV solid polymer electrolyte fuel cell: I mechanistic model development, J. Electrochem. Soc. 142 (1995) 1–8.
[36] J.C. Amphlett, R.F. Mann, B.A. Peppley, P.R. Roberge, A. Rodrigues, A model predicting transient response of proton exchange membrane fuel cells, J. Power Sources 61 (1996) 183–188.
[37] X. Yu, B. Zhou, Steady and unsteady modeling of Ballard Mark V PEM Fuel Cell Stack, CSME Forum S7 (2004) 1091–1100.
[38] B.R. Munson, D.F. Young, T.H. Okiishi, Fundamentals of Fluid Mechanics, 4th ed., 2002, p. 475.
[39] S.-H. Ge, B.-L. Yi, A mathematical model for PEMFC in different flow modes, J. Power Sources 124 (2003) 1–11.